

Net continuous wave optical gain in a low loss silicon-on-insulator waveguide by stimulated Raman scattering

Richard Jones, Haisheng Rong, Ansheng Liu, Alexander W. Fang,
and Mario J. Paniccia

Intel Corporation
2200 Mission College Blvd, CHP3-109
Santa Clara, CA 95054

Richard.jones@intel.com, Haisheng.rong@intel.com, Mario.paniccia@intel.com

Dani Hak, Oded Cohen

Intel Corporation
S. B. I. Park Har Hotzvim, Jerusalem, 91031, Israel

Abstract: We observe for the first time net continuous wave optical gain in a low loss silicon-on-insulator waveguide based on stimulated Raman scattering. We show that nonlinear optical loss due to two-photon absorption induced free carrier absorption can be significantly reduced by introducing a reverse biased p-i-n diode in the waveguide. For a 4.8 cm long waveguide with an effective core area of $\sim 1.6 \mu\text{m}^2$, we obtain a net CW Raman gain of $> 3\text{dB}$ with a pump power of $\sim 700\text{mW}$ inside the waveguide.

©2005 Optical Society of America

OCIS codes: (190.4390) Nonlinear optics, (130.0130) Integrated optics, (230.4320) Nonlinear optical devices, (230.7370) Waveguides, (250.5300) Photonic integrated circuits.

References and Links

1. H. Rong, A. Liu, R. Nicolaescu, M. Paniccia, O. Cohen, and D. Hak, "Raman gain and nonlinear optical absorption measurements in a low-loss silicon waveguide," *Appl. Phys. Lett.* **85**, 2196-2198 (2004)
2. A. Liu, H. Rong, M. Paniccia, O. Cohen, and D. Hak, "Net optical gain in a low loss silicon-on-insulator waveguide by stimulated Raman scattering," *Opt. Express* **12**, 4261-4268 (2004)
<http://www.opticsexpress.org/abstract.cfm?URI=OPEX-12-18-4261>
3. Q. Xu, V. R. Almeida, and M. Lipson, "Time-resolved study of Raman gain in highly confined silicon-on-insulator waveguides," *Opt. Express* **12**, 4437-4442 (2004)
<http://www.opticsexpress.org/abstract.cfm?URI=OPEX-12-19-4437>
4. T. K. Liang and H. K. Tsang, "Efficient Raman amplification in silicon-on-insulator waveguides," *Appl. Phys. Lett.* **85**, 3343-3345 (2004)
5. O. Boyraz and B. Jalali, "Demonstration of 11 dB fiber-to-fiber gain in a silicon Raman amplifier," *IEICE Elect. Express* **1**, 429-434 (2004)
6. G. P. Agrawal, *Nonlinear Fiber Optics*, 2nd edition (Academic Press, New York, 1995).
7. D. F. Edwards, "Silicon (Si)," in *Handbook of Optical Constants of Solids*, E. D. Palik, eds. (Academic Press, San Diego, Calif., 1998), 547-569.
8. H. K. Tsang, C. S. Wong, T. K. Liang, I. E. Day, S. W. Roberts, A. Harpin, J. Drake, and M. Asghari, "Optical dispersion, two-photon absorption and self-phase modulation in silicon waveguides at 1.5 μm wavelength," *Appl. Phys. Lett.* **80**, 416-418 (2002).
9. R. Claps, V. Raghunathan, D. Dimitropoulos, and B. Jalali, "Influence of nonlinear absorption on Raman amplification in Silicon waveguides," *Opt. Express* **12**, 2774-2780 (2004).
<http://www.opticsexpress.org/abstract.cfm?URI=OPEX-12-12-2774>
10. O. Boyraz and B. Jalali, "Demonstration of a silicon Raman laser," *Opt. Express* **12**, 5269-5273 (2004)
<http://www.opticsexpress.org/abstract.cfm?URI=OPEX-12-21-5269>
11. Details are available at <http://www.photon.com>
12. G. T. Reed and A. P. Knights, *Silicon Photonics: An Introduction* (John Wiley, West Sussex, 2004).

13. R. A. Soref and B. R. Bennett, "Electro-optical effects in Silicon," IEEE J. Quantum Electron. **QE-23**, 123-129 (1987)
14. R. A. Soref and B. R. Bennett, "Kramers-Kronig analysis of electro-optical switching in silicon," Proc. SPIE **704**, 32-37 (1986).

1. Introduction

Stimulated Raman scattering (SRS) in silicon waveguides around $1.55\ \mu\text{m}$ has recently attracted a great deal of attention [1-5] because it offers the potential of optical amplification and lasing in silicon in the optical communication bands. Silicon is attractive as it possesses a large Raman scattering coefficient which is several orders of magnitude larger than that of silica commonly used for fiber Raman amplifiers. Thus it should be possible to create chip-scale (i.e. centimeters rather than meters long) optical amplifiers [1]. Although linear optical absorption in silicon at wavelengths of $1.3\text{-}1.7\ \mu\text{m}$ is small [7], two-photon absorption (TPA) induced free carrier absorption (FCA) is a major hurdle for silicon-based Raman amplifiers due to the relatively long free carrier lifetime [1,8,9]. To overcome this problem the effective lifetime of the interaction of free carriers with the optical mode has to be reduced [4, 10]. One method of achieving this is by using optically pulsed operation, and pulsed Raman amplifiers have shown net gain [2-5] and lasing [10]. However to date there has been no demonstration of net continuous-wave (CW) optical gain in silicon.

In this paper we demonstrate the first net CW Raman gain in a silicon waveguide, i.e. Raman gain is greater than the total propagation loss. We show that the TPA induced FCA in silicon can be significantly reduced by introducing a reverse biased p-i-n junction imbedded into a silicon waveguide. With a reverse bias of 25V the carrier lifetime has been reduced to $\sim 1.0\ \text{ns}$. Using a 4.8-cm long waveguide a net CW gain of $> 3\text{dB}$ has been achieved with a pump power of $\sim 700\ \text{mW}$ inside the waveguide.

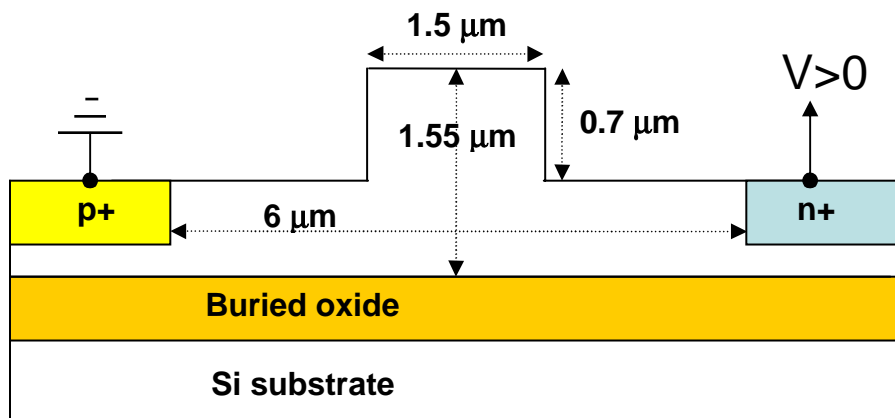


Fig. 1. Schematic diagram of the SOI p-i-n waveguide used in our experiment.

2. Device fabrication and characterization

The silicon rib waveguide is fabricated on the (100) surface of an un-doped silicon-on-insulator (SOI) substrate using standard photolithographic patterning and reactive ion etching techniques. The rib waveguide width is $1.5\ \mu\text{m}$, the rib height is $1.55\ \mu\text{m}$, and the etch depth is $0.7\ \mu\text{m}$. A schematic of the waveguide cross-section is shown in Fig. 1. The effective core area of the waveguide is calculated to be $\sim 1.6\ \mu\text{m}^2$ by using a fully vectorial waveguide modal solver [11]. A small waveguide cross-section is advantageous as it increases the pump

intensity for a given pump power and enables high Raman gain as it is the optical intensity and not power of the pump that determines the Raman scattering efficiency. To increase the interaction length, and in turn achieve larger total Raman gain, the waveguide was formed in an S-shaped curve with a total length of 4.8 cm and a bend radius of 400 μm . The straight sections of the waveguide are oriented along the [011] direction. To reduce the nonlinear optical loss due to the TPA induced FCA, a reverse biased p-i-n diode is fabricated in the waveguide. As shown in Fig. 1, the silicon rib waveguide has a heavily doped p and n type region in the slab, with a doping concentration of $\sim 1 \times 10^{20} \text{ cm}^{-3}$. The separation between the edge of the p and n type doping regions is 6 μm . Aluminium films are deposited on the p and n doped regions to form ohmic contacts. It has been experimentally verified that the presence of these doped regions and metal contacts has negligible effect on the waveguide loss; which is due to the tightly confined mode for the waveguide being used. The linear optical transmission loss of the S-bend waveguide is $0.4 \pm 0.1 \text{ dB/cm}$; measured using the Fabry-Perot resonance technique [12] prior to anti-reflection coating the silicon waveguides. The 0.1 dB/cm uncertainty in the linear optical loss includes the experimental error and waveguide-to-waveguide variations.

3. Experimental results and analysis

When a reverse bias is applied to the p-i-n diode, the TPA-generated electron-hole pairs can be swept out of the silicon region between the p- and n-doped regions, where the optical mode is located. If the carrier transit time across the optical mode area is shorter than the free carrier lifetime, then the transit time becomes the effective carrier lifetime. This effective carrier lifetime, which is associated with the free carrier's interaction with the optical mode, determines the TPA induced carrier density. By varying the reverse bias voltage, the carrier transit time and hence effective carrier lifetime can be modified. In the CW pumping case, the free carrier density induced by the TPA is given by [1, 2]

$$N(z) = \frac{\tau\beta}{2hv} \frac{P^2(z)}{A_{eff}^2} \quad (1)$$

where β is the TPA coefficient, $P(z)$ is the pump power along the waveguide, A_{eff} is the effective core area of the waveguide, hv is the one-photon energy of the pump beam, and τ is the effective carrier lifetime. Taking into account both the TPA and TPA induced FCA, the pump power evolution along the waveguide is described by the following equation [1,2]

$$\frac{dP(z)}{dz} = -\alpha P(z) - \frac{\beta}{A_{eff}} P^2(z) - \sigma N(z)P(z) \quad (2)$$

where α is the linear absorption coefficient and σ is the free carrier absorption cross section. As is evident from Eq.(1), the free carrier density can be reduced if the carrier lifetime τ in the waveguide region is shortened. In turn, the FCA will also be reduced. To experimentally verify this, we measured the transmitted pump power versus input power for a 4.8 cm long S-shaped silicon p-i-n diode waveguide with AR coatings applied to both facets for various reverse bias voltages. Results are presented in Fig. 2. The symbols represent the measured results and the solid curves are the modelled results by solving combined Eqs. (1) and (2). Fig. 2 indicates that there is a good agreement between modeled and measured results for various reverse bias voltages. As can be seen in Fig. 2, at low input powers the output power is linearly dependent upon the input power. As the input power is increased above 200 mW, the output power saturates, with the saturated output power depending upon the p-i-n diode bias. For an open circuited p-i-n waveguide, the output power saturates to a constant value of $\sim 180 \text{ mW}$ independent on the input power. Short-circuiting and reverse biasing the p-i-n structure allows current to flow, which removes the free carriers from the optical mode and reduces the

effective carrier lifetime, thus increasing the output intensity. This demonstrates that reduction in the FCA is achievable with this device structure.

By comparing the modeling and experiment, we can determine the effective carrier lifetime in the p-i-n diode waveguide. As the carrier lifetime depends on the reverse bias voltage, we use it as a fitting parameter. Other parameters used in the modelling are the linear absorption coefficient of $\alpha=0.39$ dB/cm, the previously reported TPA coefficient of $\beta=0.5$ cm/GW [1,2], and the FCA cross section of $\sigma=1.45\times 10^{-17}$ cm² [13] at a wavelength of 1.55 μ m. When the p-i-n diode is open (no current flow is allowed), the modelled carrier lifetime is ~ 16 ns. When the p-i-n diode is short circuited (external bias is zero but current flow is possible due to the internally built-in potential of the p-i-n), the carrier lifetime is much shorter ($\tau=6.8$ ns). By increasing the reverse bias voltage, the carrier lifetime is further reduced, and at a reverse bias of 25 V, an effective carrier lifetime of ~ 1 ns is obtained.

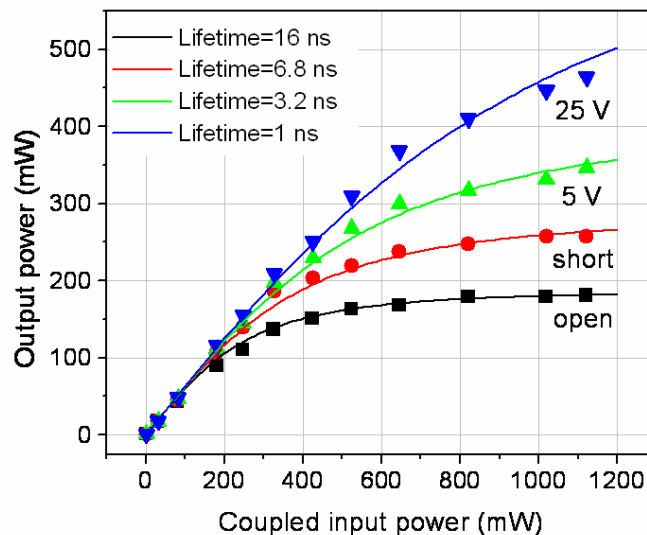


Fig. 2. Measured and modeled output power as a function of the input power for a 4.8 cm long waveguide containing a reverse biased p-i-n diode with various bias voltages. Symbols represent the experimental data and curves are the modeled results. The carrier lifetime is used as a fitting parameter for each bias voltage.

To measure the gain of the silicon waveguide containing a p-i-n diode, we performed a pump-probe experiment. The experimental setup is shown in Fig. 3. The pump and probe lasers are combined with a wavelength multiplexer into a lensed single-mode fiber whose output is used to couple to the waveguide under investigation. The output beam of the waveguide is collimated by a 50 \times objective lens, and a long-wavelength pass optical filter is used to separate the pump and probe beams. The probe beam passes through the filter and is detected with a photo-detector while the pump beam is blocked by the filter. Fiber polarization controllers at the input to the device under test allow both probe and pump beam polarizations to be independently controlled. The device under test is mounted on a TEC and kept at a constant temperature of 25 $^{\circ}$ C.

For the CW gain measurements, the pump laser is a CW tunable external cavity laser emitting around 1548.3 nm, which is amplified using two EDFA's to a maximum output power of 4 W. The probe laser is a 2 mW, external cavity tunable diode laser operating at around 1684 nm. Both the pump and probe laser sources have line-widths of ≤ 100 MHz. The polarization of the probe and the pump beam are aligned with the TE mode of the waveguide.

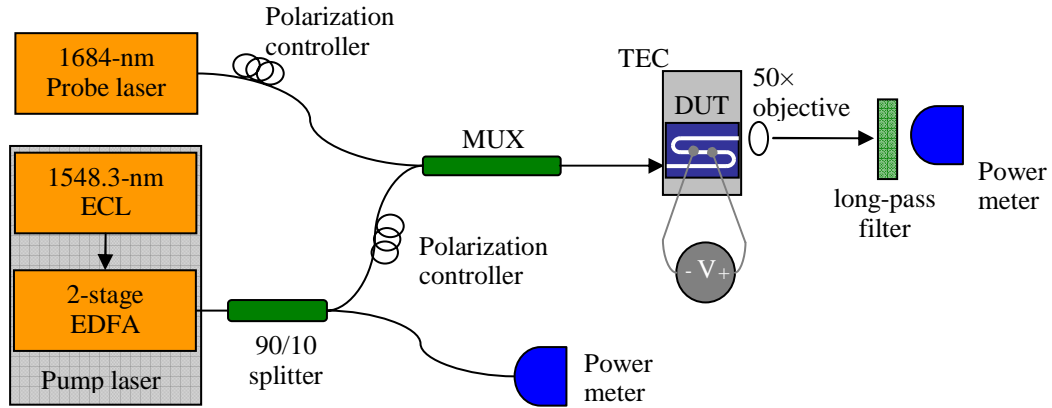


Fig. 3. Experimental setup of CW gain measurement, DUT is device under test

To measure the SRS gain, the transmitted probe power is measured at the peak of the Raman gain profile (at the Stokes wavelength) and compared to the input probe power. The input probe power is determined from the measured transmitted probe power without the pump beam by factorizing out the linear transmission loss of the waveguide.

Since the probe power is low, we ignore the pump depletion in the description of the pump-probe experiment. Taking into account the TPA and TPA induced FCA at the Stokes wavelength, the probe power $[P_s(z)]$ in the waveguide can be described by [2,6]

$$\frac{dP_s(z)}{dz} = -\alpha P_s(z) - \frac{2\beta - g_r}{A_{eff}} P(z)P_s(z) - \sigma N(z)P_s(z) \quad (3)$$

where g_r is the Raman gain coefficient. Solving Eq. (3) using the pump power obtained from Eq. (2) and with probe input power $P_s(0)$ as an initial condition, one obtains the net optical gain of the waveguide via

$$G = 10 \log \frac{P_s(L)}{P_s(0)} \quad (4)$$

where $P_s(L)$ is the probe output power obtained from Eq. (3), and L the waveguide length.

Fig. 4 shows the net CW Raman gain as a function of the pump power inside the waveguide for a 4.8 cm long waveguide at various bias voltages. The pump power is the power of the pump coupled into the waveguide, and is determined by measuring the power exiting the lensed fiber and factorizing out coupling loss to the waveguide. The symbols represent the experimental data and the curves are the modeled results. In the modeling, we used a linear loss of 0.39 dB/cm. At the Stokes wavelength, the FCA cross section is $1.71 \times 10^{-17} \text{ cm}^2$ [14]. Since the same waveguide was used for both the nonlinear transmission and pump-probe measurements, the corresponding carrier lifetime shown in Fig. 2 were used in the simulation of the net gain in Fig. 4. The only fitting parameter is the gain coefficient g_r . We see from Fig. 4 that there is no net gain when the p-i-n diode is open. This is because, when the carrier lifetime is long, the Raman gain can't compensate for the loss due to the linear waveguide scattering loss, TPA, and TPA induced FCA. When the diode is short circuited, the FCA is significantly reduced, but there is still no net gain observed. Once the p-i-n is reverse biased net gain is achieved. With a reverse bias of 5 V, we obtained a net gain of ~2 dB with a pump power of ~700 mW. Using a higher bias voltage of 25 V, a net gain of >3 dB is achieved for pump powers above 700 mW. To the best of our knowledge, this is the first demonstration of net CW Raman gain reported in silicon. From Fig. 4 we see that

experimental data agrees relatively well with modeling results based on a gain coefficient of $g=9.5$ cm/GW.

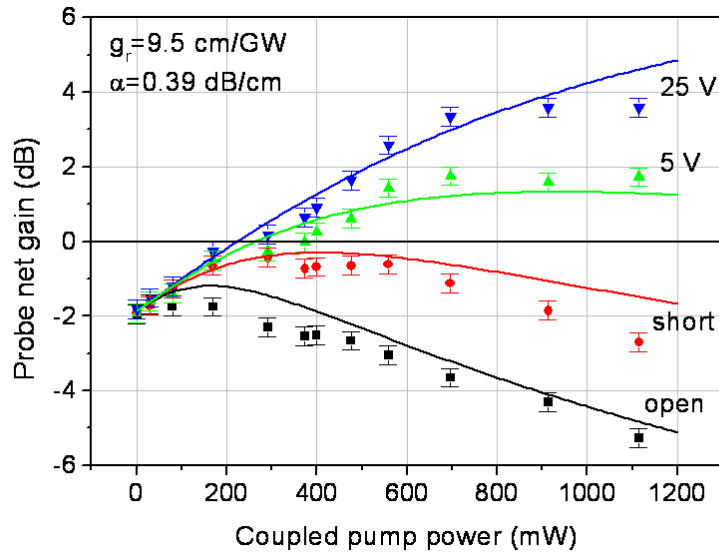


Fig. 4. Net Raman gain for a p-i-n diode embedded in a silicon waveguide as a function of the pump intensity for a 4.8 cm long silicon waveguide at different bias voltages. Symbols represent the experimental results and solid curve is the modeling result. The Raman gain coefficient used in the simulation is $g_r=9.5$ cm/GW.

Fig. 5 shows the net Raman gain, at a probe wavelength of 1684 nm, as a function of the pump wavelength. The p-i-n bias was set at 25 V and the pump power at 511 mW. For this configuration net Raman gain is observed over 0.5 nm. Fig. 5 also shows that the 3 dB linewidth of the SRS spectrum is ~ 100 GHz.

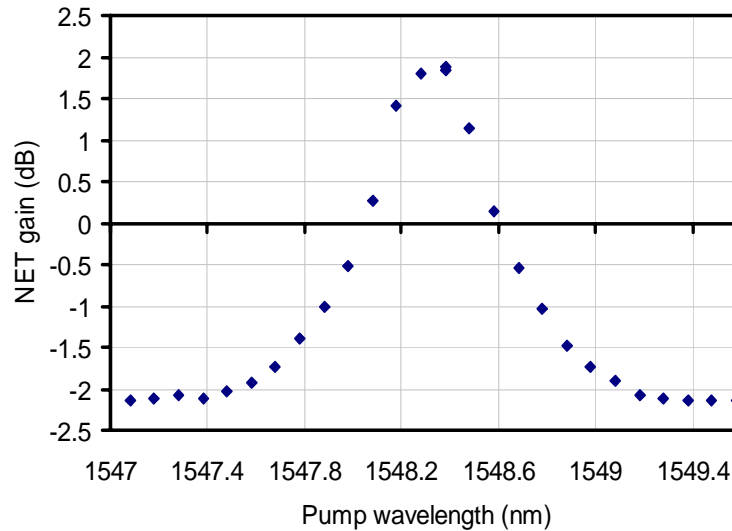


Fig. 5. Net Raman gain as a function of the pump wavelength for a 4.8 cm long silicon waveguide. The pump power is 511 mW, the probe wavelength is 1684 nm, and the reverse bias on the p-i-n is 25 V.

4. Conclusion

In conclusion, we have achieved for the first time net CW optical gain in a silicon waveguide via stimulated Raman scattering. We have demonstrated the effective free carrier lifetime and hence TPA induced FCA can be reduced using a reverse biased p-i-n embedded in a silicon waveguide. A reduction of the free carrier lifetime from 16 ns to 1 ns has been achieved. For a waveguide of 4.8 cm, a net CW gain of > 3 dB is obtained with a pump power of ~ 700 mW inside the waveguide with a reverse bias of 25V. The achievement of net CW optical gain in silicon is an important step in being able to achieve CW lasing, and producing active devices in silicon.

Acknowledgments

The authors thank R. Nicolaescu for initiating and developing this research through the early stages; J. Tseng and D. Tran for assistance in device fabrication and sample preparation; S. Koehl for data collection software development; and M. Morse, D Samara-Rubio, and G. T. Reed for helpful discussions.